SLAC-TN-73-1 (Revised)
C. Y. Prescott
January 1973

SPIN DEPENDENT COMPTON SCATTERING FOR USE IN ANALYZING ELECTRON BEAM POLARIZATIONS

I. Introduction

The application of back scattering of laser light to provide highly polarized beams of photons for photoproduction experiments is well documented[1] and has been highly successful in bubble chamber experiments at SLAC. It is the purpose of this note to look again at this process with particular attention paid to the spin dependent parts of the cross section which can serve to analyze polarizations of incident high energy electrons. Effects which depend on the incident electron polarization are seen in the angular distributions, energy spectra and total cross sections. In particular, the total cross section for incident electrons having spins parallel to the spins of incident photons is larger than that of the corresponding antiparallel configuration. The size of the difference increases with the center-of-mass energy. One can use the spin dependence of the cross section to measure the incident electron polarization (assuming the photon polarization is known) by comparing the rate of back scattered photons for the two spin configurations. However, we observe that if one sums over the energies of scattered photons, rather than just counting the number of back scattered photons, one obtains a more sensitive measure of the electron spin. (See Section IV.)

Measurement of the back scattered laser energy is readily accomplished. One places a total absorption shower counter (TA) in the beam of the back scattered laser photons. A properly designed TA counter responds linearly to the energy of incident photons. Furthermore, one can measure the energy of many photons at once, without counting each photon individually, since the response of the device is linear. This is important to a test because the laser produces a "burst" of photons in a short pulse ($\sim$ 80 nsec). By counting many photons at once, one can obtain good statistical accuracy in relatively short times.

Revised March 1973.

Circularly polarized light can be generated by inserting a 1/4-wave plate in the linearly polarized laser light, and suitably orienting it. The spin configuration can be changed from parallel to antiparallel (i.e., the photon spin can be reversed) by rotating the 1/4-wave plate by 90 degrees. During the data taking, the spin of the photon will be reversed often, up to once per second, so that drifts in the system will be averaged out.

Figure 1 shows a suitable experimental arrangement for a test. A TA counter is placed in the laser beam in front of the 82" bubble chamber. A lead aperture of 30 cm diameter permits nearly all scattered photons to enter the counter aperture. A scintillation hodoscope in front of the TA counter permits monitoring of the steering of the laser beam during the tests. The TA counter output is processed separately in a pulse-height-analyzer, according to whether the spin orientations are parallel or antiparallel.

The analysis of the data is simple. One forms a ratio

$$R = \frac{\text{Energy (parallel spins)}}{\text{Energy (antiparallel spins)}}$$

$$= \frac{\Sigma \ \text{TA response (parallel)}}{\Sigma \ \text{TA response (antiparallel)}}$$

which is independent of beam normalization. This ratio should be about .86 for 20 GeV electrons in the laser beam line, and the accuracy for measuring the electron polarization depends on how well one measures the difference of this value from 1.0.

In the following sections we analyze the Compton scattering process. In Section V we study one of the processes that contributes to the radiative corrections. For the case where two photons emerge in the final state (double Compton scattering) we find that the influence is negligibly small. Section VI looks at specific considerations for the C-beam line; most notably these are the precession of electron spin, and the expected counting rate for back scattered laser photons.

II. Kinematics

We review here the basic kinematics of Compton scattering. The analysis here uses the parametrization of Ref. 1. In the frame in which the electron is at rest, the familiar Compton formula is

$$\frac{m}{K} - \frac{m}{K_0} = 1 - \cos\theta_0$$

where K_0 and K are the energies of the incident and scattered photons, and θ_0 is the angle of the scattered photon relative to the incident photon.

In the laboratory frame, the electron is moving with velocity β and has energy $E = \gamma m$. The back scattered photons have an energy K_f and for $\cos\theta_0 = -1$, reach a maximum value, $K_{f\,max}$.

$$K_{f\,max} = E(1-a) = 4a\,\gamma^2 K_i$$

where

$$a = (1 + 4\,\gamma\,K_i/m)^{-1}$$

$$K_i = \text{incident photon energy in lab.}$$

We define a dimensionless parameter

$$\rho = K_f/K_{f\,max} \cong \left[1 + a(\gamma\theta)^2\right]^{-1}$$

where θ now measures the direction of the scattered photon relative to the incident electron direction, and the approximation $\theta \cong 2 \tan\theta/2$ has been used.

For a study of the spin dependence of Compton scattering, we refer to the work of Lipps and Tolhoek[2]. The terms of interest here are the correlations between incident photon spin and incident electron spin. If we exclude the cases where final state particle polarizations are observed, the only spin-dependent terms of interest in the cross section arise from circularly polarized photons scattering off polarized electrons.

Let the frame of reference be the one at rest with the incident electron. The Z-axis is chosen along the direction of incoming electrons, and the spin of the electron lies in the X-Z plane, with a component $P_e \cos \Psi$ along the Z-axis, and $P_e \sin \Psi$ along the X-axis (see Fig. 2).

The photon has circular polarization P_γ. The scattered photon has a polar angle θ_0 and an azimuthal angle ϕ.

The Compton cross section is

$$\frac{d\sigma}{d\Omega} = \tfrac{1}{2} r_0^2 K^2/K_0^2 \left[\frac{(K_0-K)^2}{K\ K_0} + 1 + \cos^2\theta_0 \right.$$

$$\left. \mp \left\{ (K/K_0 - K_0/K)\, P_\gamma P_e \cos\Psi \cos\theta_0 + (1 - K/K_0)\, P_\gamma P_e \sin\Psi \sin\theta_0 \cos\phi \right\} \right]$$

The - sign is chosen for the case of the longitudinal component of the photon spin parallel to its direction of motion[4].

Transforming to the laboratory frame, and expressing the cross section in terms of the dimensionless parameter ρ, one obtains

$$\frac{d^2\sigma}{d\rho d\phi} = \frac{d^2\sigma_0}{d\rho d\phi} \mp P_e P_\gamma \left\{ \cos\Psi \frac{d^2\sigma_1}{d\rho d\phi} + \sin\Psi \cos\phi \frac{d^2\sigma_2}{d\rho d\phi} \right\}$$

where

$$\frac{d^2\sigma_0}{d\rho d\phi} = r_0^2 a \left\{ \frac{\rho^2(1-a)^2}{1-\rho(1-a)} + 1 + \left(\frac{1-\rho(1+a)}{1-\rho(1-a)} \right)^2 \right\}$$

$$\frac{d^2\sigma_1}{d\rho d\phi} = r_0^{\,2}a \left\{ (1 - \rho(1+a))\,(1-1/(1-\rho(1-a))^2) \right\}$$

$$\frac{d^2\sigma_2}{d\sigma d\phi} = r_0^{\,2}a \left\{ \rho(1-a)\ \sqrt{4a\rho(1-\rho)}\,/\,(1-\rho\,(1-a)) \right\}$$

The last term represents an azimuthal dependence in the cross section. This term can arise because the transverse component of the electron spin breaks the azimuthal symmetry in the scattering process. If one averages over all ϕ angles, this term vanishes. Similarly, if the incident photon has linear polarization components mixed with the circular polarization, azimuthal dependence will occur in the cross section. For our purpose, we study the energy dependence of the cross section integrated over all ϕ. Since the reaction is two-body, the energy of the scattered photon is directly related to its polar angle, so this approach is equivalent to an angular distribution.

III. Differential Cross Sections

The cross section per unit energy for the scattered photon, integrated over the azimuth ϕ is

$$\frac{d\sigma}{d\rho} = \frac{d\sigma_0}{d\rho} \mp P_e P_\gamma \cos\Psi \ \frac{d\sigma_1}{d\rho}$$

Figure 3 shows the ρ dependence for $d\sigma_0/d\rho$ and $d\sigma_1/d\rho$. The curves are plotted for ruby laser photons incident or 10 GeV electrons (denoted "B10" for blue photons on 10 GeV electrons) and similarly for 20 GeV incident electrons. The parameter "a" depends on the product E_0 (electron) K_i (photon), so that R20 and B10 curves are the same. The term which gives rise to a cross section asymmetry is $d\sigma_1/d\rho$. This asymmetry is largest at $\rho = 1$, corresponding to back scattered photons. If one selects photons of a definite energy ρ and measures the asymmetry in the counting rate as the helicity of either the electron or photon is flipped (but not both), one has

$$\text{Asymmetry} = A = \frac{N_+(\rho)-N_-(\rho)}{N_+(\rho)+N_-(\rho)} = -P_e P_\gamma \cos\Psi \frac{d\sigma_1/d\rho}{d\sigma_0/d\rho} \quad .$$

The quantity

$$\epsilon\ (\rho) = d\sigma_1/d\rho/d\sigma_0/d\rho$$

is plotted in Fig.4. One sees that the tip of the spectrum, $\rho = 1$, is the most sensitive to the spin dependent terms.

IV. Back Scattered Energy Spectrum

If we wish to measure the energy scattered backward into an aperture, we must consider the number of photons (proportional to $d\sigma/d\rho$) weighted by the energy ρ. That is

$$\epsilon\ (\rho) = \rho d\sigma/\, d\rho = \rho\ d\sigma_0/d\rho \mp P_e P_\gamma \cos\Psi\ \rho\ d\sigma_1/d\rho$$

This is of experimental interest, because it weights more heavily those parts of the spectrum which are more sensitive to the spin dependent terms.

The energy of back scattered photons is measured by a total absorption shower counter. Because of the Lorentz transformation from the electron rest frame to the laboratory frame, a typical shower counter aperture (say 30 cm diameter circle, for example) will detect essentially all scattered photons. If one restricts the aperture by collimation, the sensitivity to beam steering and wandering is increased, and counting rate is lost. Counting of several photons separately in the short burst (~ 80 nsec) is probably not possible. The most straightforward procedure is to measure the energy of <u>all</u> scattered photons contained within a single pulse on a pulse to pulse basis. If we define a quantity R to be the ratio of energies scattered into the counter aperture for parallel vs antiparallel configuration of spins, then

$$R(P) = \frac{\int_0^1 \rho(d\sigma_0/d\rho - P\ \ d\sigma_1/\, d\rho)d\rho}{\int_0^1 \rho(d\sigma_0/d\rho + P\ \ d\sigma_1/\, d\rho)d\rho}$$

where $P = P_\gamma P_e \cos\Psi$. Here we take P_e to be the polarization emerging from the linear part of the accelerator, and precession of the spin direction due to switch yard and beam line bending magnets is accounted for by the cos Ψ factor (see Section VI.)

The dependence of R on P is not linear, but there is a one-to-one correspondence so that measurement of R(P) yields a value of P. Knowing the survey parameters for the beam line allows cos Ψ to be calculated, so that P_e can be determined. The statistical accuracy of a measurement of R depends on the counting rate. However, the procedure suggested above allows one to count many photons per pulse, so that the accuracy of the measurement R will probably be controlled by systematic effects (false asymmetries) rather than by counting statistics.

Fig. 5 shows the dependence of R on P, for the cases of red laser light on 10 GeV incident electrons. Frequency doubled blue laser light on 10 GeV incident electrons, and the same for 20 GeV electrons.

V. Radiative Corrections

The radiative corrections considered here are those terms which contribute to the emission of an energetic photon. The first order correction to single Compton scattering arises from internal photons connecting electron lines, bubbles in the external photon lines and from emission of two photons from electron lines. The proper spin-dependent treatment including these first order corrections is a not-so-trivial problem. It is presently being studied. To obtain an estimate of the size of the terms involved, the process of two photon emission is considered by itself. Only the spin-independent term is considered. The differential cross section for double Compton scattering can be written[3]

$$d\sigma_{DC} = \frac{\alpha r_0^2}{16\pi^2} \iiint f(K_0, K_1, \theta, \phi, \theta_C, \phi_2) dK_1 d\Omega_1 d\Omega_2$$

where f is a known function, and dependence on K_2 has been removed by energy momentum conservation.

Numerical integration of this formula is straightforward. The integrals diverge, however as $K_1 \rightarrow 0$. This is the well known infra-red divergence, which is handled in a proper treatment by cancelling the divergent terms with other equally divergent terms from the radiative corrections to single Compton scattering. Here we choose a lower limit for K_1. It seems reasonable that the radiative processes could "wash out" spin dependent effects only if the resulting integrals are a sizeable part of the single Compton cross section. Table I gives the values $\sigma_{DC}(K > K_{min})$ for several values of K_{min}. Because of the small size of these terms, it appears reasonable to proceed on the basis of formulae from the lowest order single Compton process alone.

TABLE I

Total Cross Sections for Double Compton Scattering for Both Final Photons > K_{min}

K_{min}/K_0	E_0	Laser	σ_{DC}	σ_{DC}/σ_{SC}
.025	10	Red	.11 mb	2.0×10^{-4}
.025	20	Red	.31 mb	6.8×10^{-4}
.05	10	Red	.08 mb	1.5×10^{-4}
.05	20	Red	.21 mb	4.6×10^{-4}
.1	10	Red	.05 mb	9.4×10^{-5}
.1	20	Red	.13 mb	2.8×10^{-4}

VI. Use of the C-Beam Laser Facility

It is relatively easy to perform a test of electron beam polarization in the presently existing laser facility in the SLAC C-beam area, particularly if one compares it to the effort required to provide a laser beam in the ESA beam line. The following are some of the considerations involved in using the C-beam.

1) As electrons pass through magnetic fields, the spin direction precesses faster than the momentum direction by an amount

$$\Psi_{prec} = \gamma \left(\frac{g-2}{2}\right) \theta_{bend}$$

where $\gamma = E/m$ for the electron,

and $\frac{g-2}{2} = .001597.$

The angle of bend for the electrons passing through the C-beam magnets is 4.5 mrad vertical deflection and 2.65 degrees horizontal deflection. Fig. 6 shows the factor cos Ψ_{prec} as a function of the incident energy. At E_0 = 14.97 GeV, the electron spin has precessed 90^o and cannot be measured by the techniques of Section IV. Good measurements should be possible, however, below 10 GeV and around 20 GeV.

2) Circular polarization of laser light is obtained by insertion of a 1/4-wave plate, properly oriented, in the linearly polarized laser beam. The helicity can be flipped by rotating the 1/4-wave plate 90^o.

3) The quality of the measurements will depend critically on the ability to minimize false asymmetries.

One can test for false asymmetries in the following ways:

a) Back scatter off normal unpolarized electrons obtained from the regular injection gun rather than from the polarized electron source.

b) Measurements at E_0 = 15 GeV, where electron spins are transverse, should yield no real asymmetries.

c) Orientation of the 1/4-wave plate so that it passes the linear polarization undisturbed. (This can be done by rotating it 45^o to its usual orientation.) The resulting linear polarization will generate azimuthal dependence in the cross section but no asymmetries when averaged over azimuth.

4) Counting rate estimates are obtained by use of the formula*

$$Y = \frac{1}{2} \times \frac{2 n_1 n_2 \sigma \ell}{A c \tau}$$

where

n_1 = number of incident γ's/pulse = 3.5×10^{18}

n_2 = number of incident electrons/pulse = 1×10^9

σ = effective cross section into aperture = 430 mb

ℓ = length of interaction region = 500 cm

* The factor $\frac{1}{2}$ is introduced to account for beams crossing at 3 mrad. These numbers given here are for red laser photons scattering on 20 GeV incident electrons.

A = area of largest beam = 1 cm^2

τ = length of longer pulse duration = 1.5×10^{-6} sec

One obtains a value of

$Y \approx 17$/pulse.

Since the scattered photons carry about 3.5 GeV average energy, the measurement of the scattered energy for each photon will be very good (accurate to a few percent). The measurement of Y will depend mostly on the statistical fluctuation in the number of scattered photons seen. The statistical accuracy of short runs will be good.

5) For 20 GeV incident electrons the ratio R for energies scattered for the parallel configuration vs anti-parallel configuration is .866. At 10 GeV the corresponding ratio is 1.096. (The sign of P has changed because of precession of the electrons in the C-beam magnets, causing the ratio R to change from < 1 to > 1.) The ability to measure P_e is determined by how well one measures the deviation of R from 1, i.e., how well one can measure a 13% effect. Because the counting rate is expected to be relatively good, statistical accuracy will be easy to achieve.

REFERENCES

1. J. J. Murray and P. R. Klein, SLAC-TN-67-19, June 1967; also C. K. Sinclair, J. J. Murray, P. R. Klein, M. Rabin, I. E. E. E. Trans. on Nuclear Science 16, No. 3, 1065 (1969). Earlier references are given in these reports.
2. F. W. Lipps and H. A. Tolhoek, Physica 20, 85, 395 (1954). (In equation 2.7, pg. 397, the factor k cos θ should be k_0 cos θ.) For a general discussion of spin dependent Compton scattering, see S. Gasiorowicz, Elementary Particle Physics (J. Wiley and Sons, New York, 1967); Chapter 10.
3. J. M. Jauch and F. Rohrlich, Theory of Photons and Electrons (Addison-Wesley Publishing Company, Inc., Reading, Mass., 1955); Chapter 11.
4. The quantities P_e, P_γ here are taken to be positive. The sign for P_e is incorporated in the cos Ψ term, and is positive for electron spins along the incident electron direction. For incident circularly polarized photons with spin projections along the direction of motion, choose the "-" sign. This corresponds to an electric field $\vec{E} = E_0 (\hat{e}_x + i\,\hat{e}_y)\, e^{i(Kz-\omega t)}$. See J. D. Jackson, Classical Electrodynamics (J. Wiley and Sons, New York, 1967); Chapter 16.

FIGURE CAPTIONS

1. Schematic layout of test in C-beam. Back scattered laser photons enter aperture of the total absorption shower counter, causing shower development. Integrated output (i.e., total charge) is proportional to total energy contained in all photons seen in that 1.5 μsec long pulse. Hodoscope distributions in two dimensions will be monitored during setup and running to aid in beam steering. The laser photon spins will be reversed often (up to once per second), and separate pulse height spectra for each spin configuration will be recorded.
2. Coordinate system used. The spin of the electron lies in the X-Z plane, rotated an angle Ψ relative to the Z axis. The scattered photon recoils at an angle $\pi-\theta_0$ relative to the incoming electron direction, which is the + Z axis and at an azimuthal angle ϕ.
3. The differential cross sections $d\sigma/d\rho$. The spin independent part $d\sigma_0/d\rho$ and the spin dependent part $d\sigma_1/d\rho$, averaged over ϕ, are shown for the cases:
    1) red laser light on 10 GeV electrons (R10),
    2) red laser light on 20 GeV electrons (R20),
    3) frequency doubled blue laser light on 10 GeV electrons (B10),
    4) frequency doubled blue laser light on 20 GeV electrons (B20).
4. The asymmetry parameter $\epsilon = d\sigma_1/d\rho/d\sigma_0/d\rho$ is given for the 4 cases R10, R20, B10, B20.
5. The parameter R(P), where R is ratio of back scattered energy for the parallel vs antiparallel configuration

$$R = \frac{\text{Energy (parallel)}}{\text{Energy (antiparallel)}}$$

6. Precession factor cos Ψ for the C-beam. Incident electrons become transverse at $\sim$15 GeV. At 10 GeV, the precession is $\sim 60.1^\circ$, and at 20 GeV 120.2° resulting in a change of sign for the quantity $P_e P_\gamma \cos\Psi$ between these two energies.

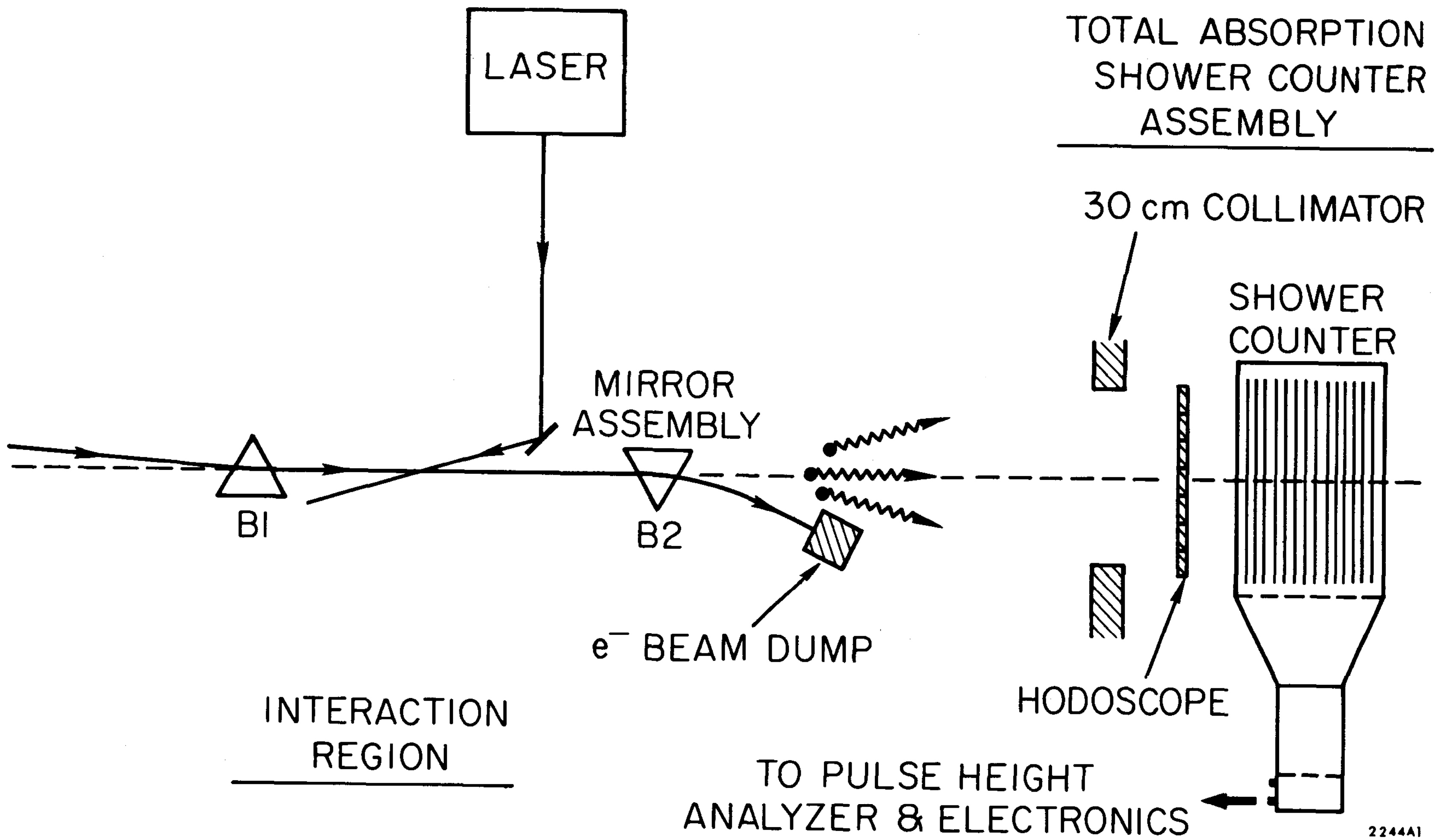
LASER
TOTAL ABSORPTION
SHOWER COUNTER
ASSEMBLY
30 cm COLLIMATOR
SHOWER
COUNTER
MIRROR
ASSEMBLY
B1
B2
e⁻ BEAM DUMP
INTERACTION
REGION
HODOSCOPE
TO PULSE HEIGHT
ANALYZER & ELECTRONICS
2244A1

Figure 1

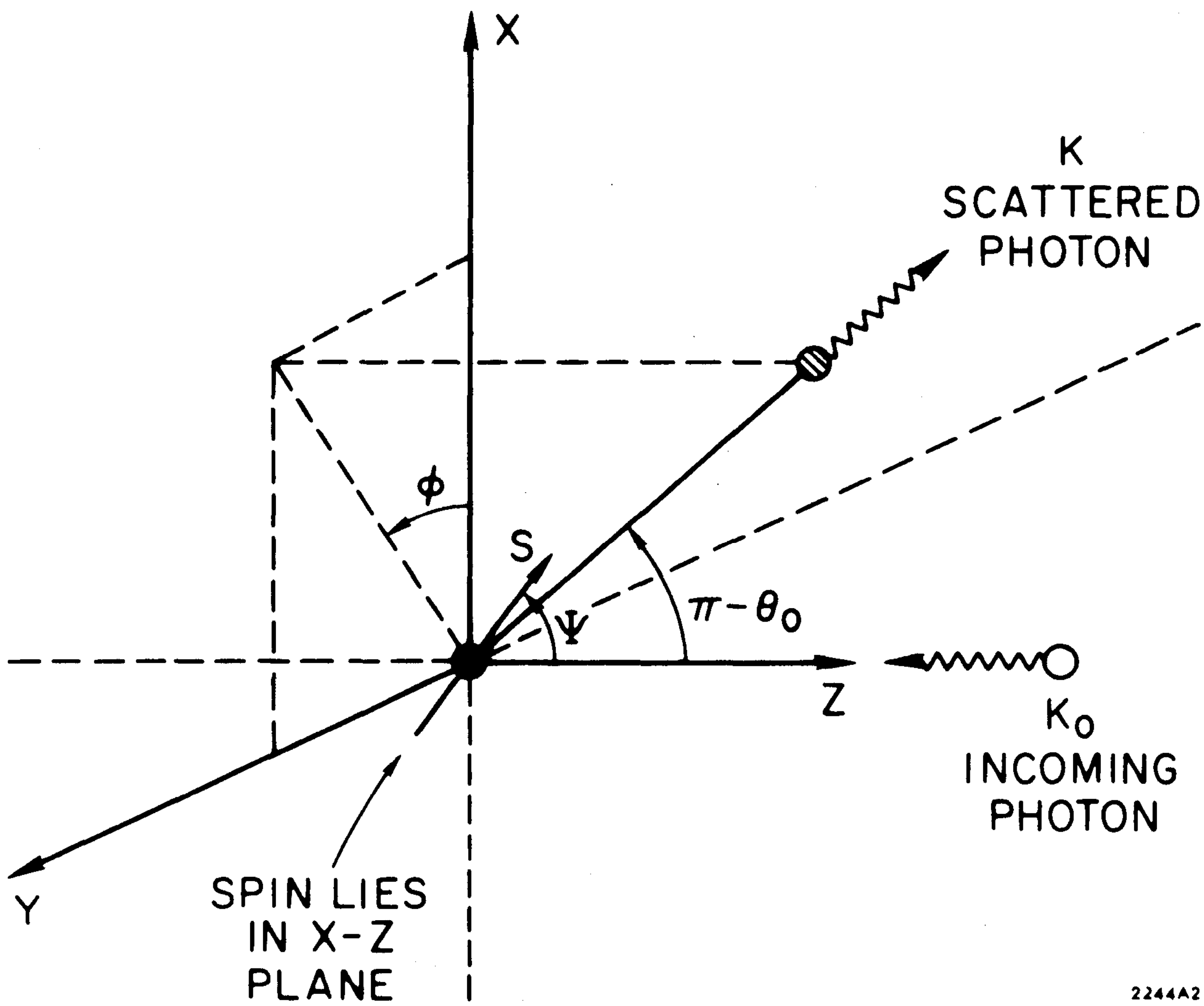
X
K
SCATTERED
PHOTON
φ
S
Ψ
π − θ0
Z
K0
INCOMING
PHOTON
Y
SPIN LIES
IN X-Z
PLANE
2244A2

Figure 2

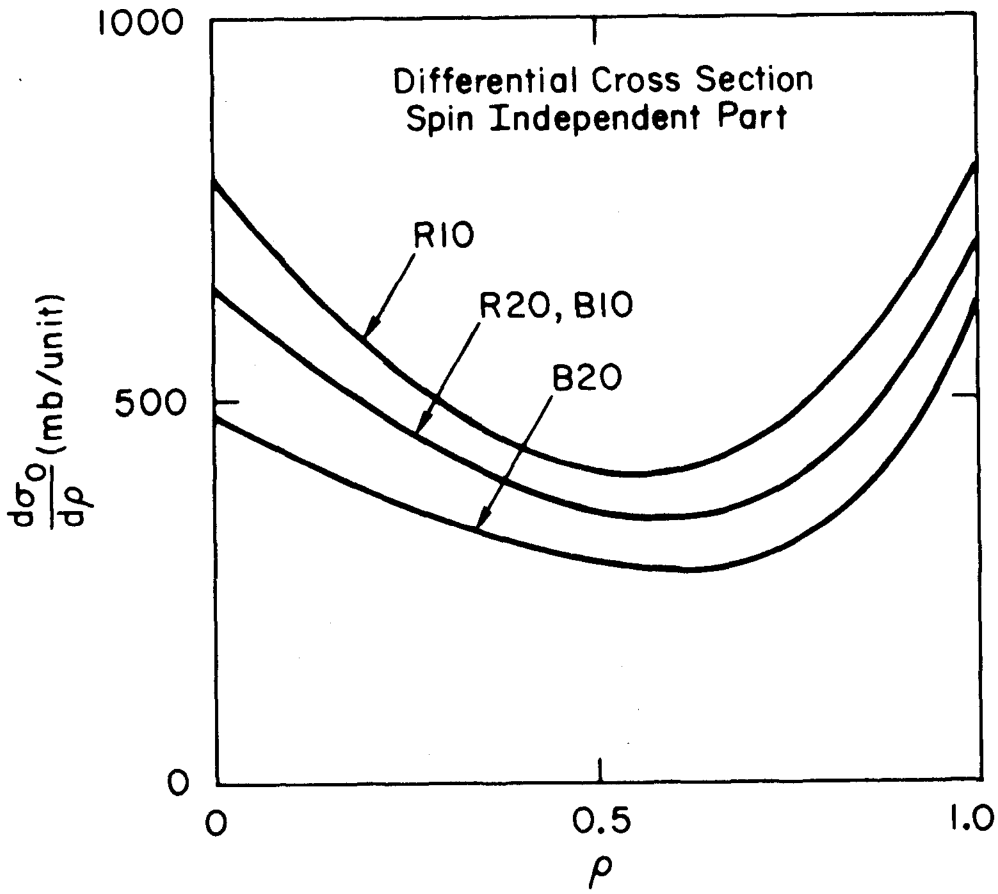
Differential Cross Section
Spin Independent Part
R10
R20, B10
B20
1000
500
0
0
0.5
1.0
ρ
dσ0/dρ (mb/unit)

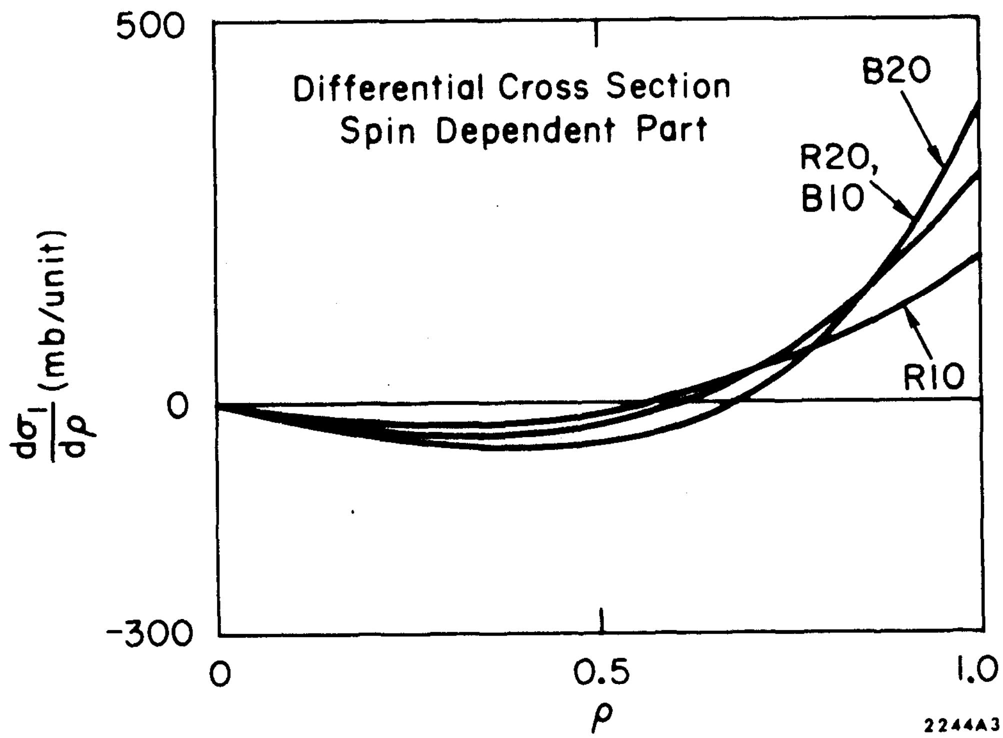
Differential Cross Section
Spin Dependent Part
B20
R20,
B10
R10
500
0
-300
0
0.5
1.0
ρ
dσ1/dρ (mb/unit)
2244A3

Figure 3

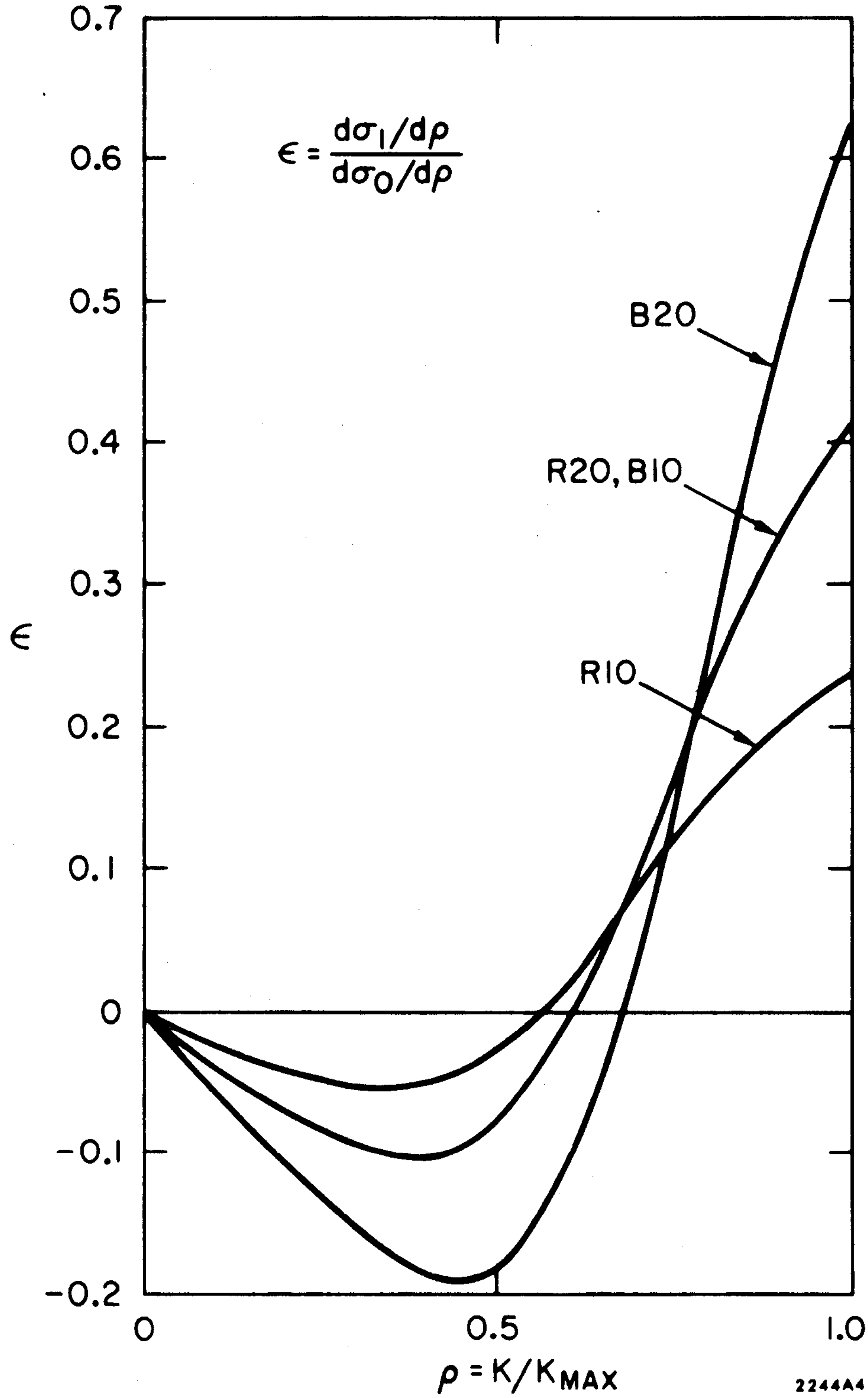
0.7
0.6
0.5
0.4
0.3
0.2
0.1
0
-0.1
-0.2
$\epsilon = \frac{d\sigma_1/d\rho}{d\sigma_0/d\rho}$
ϵ
B20
R20, B10
R10
0
0.5
1.0
$\rho = K/K_{MAX}$
2244A4

Figure 4

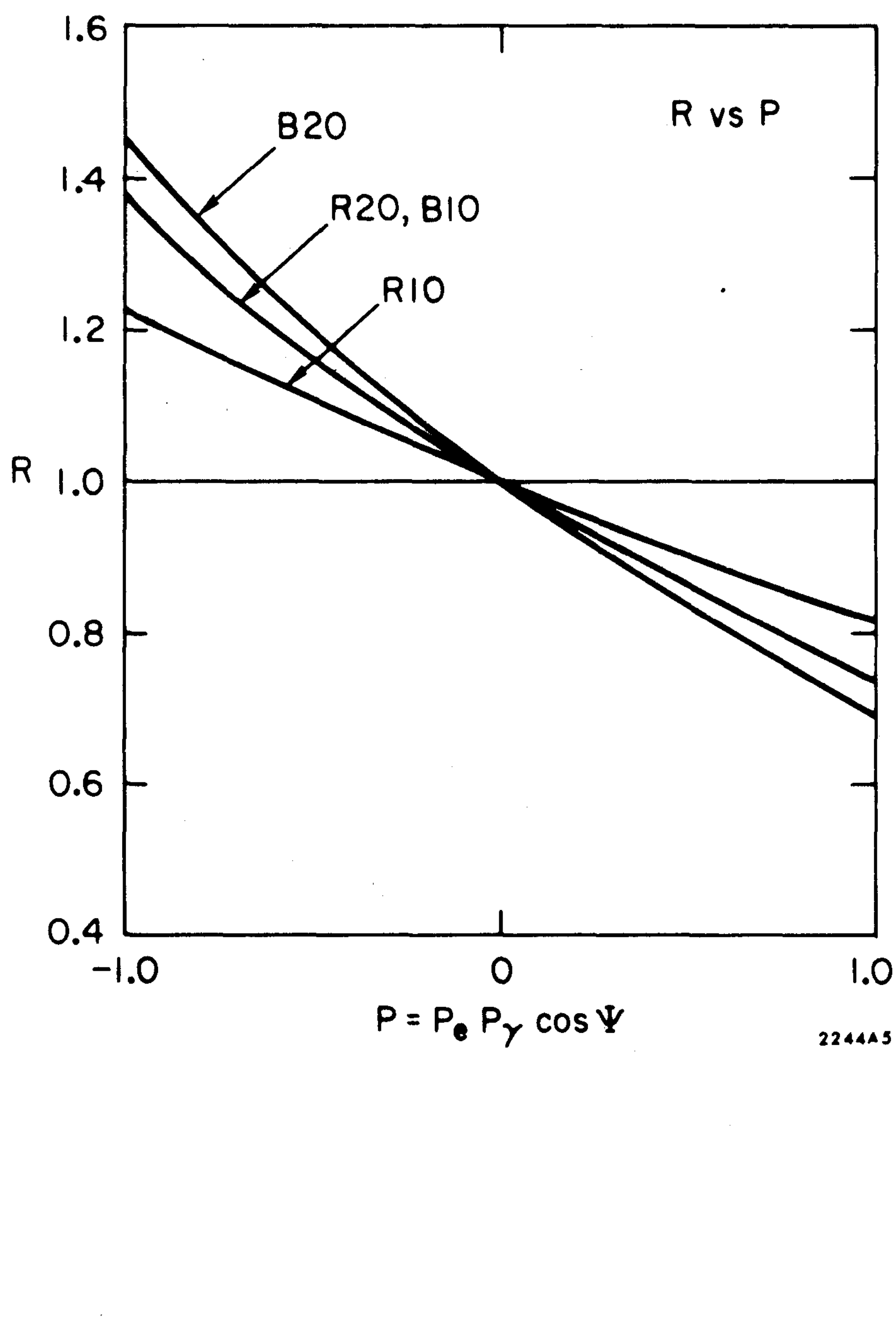

R vs P
B20
R20, B10
R10
R
1.6
1.4
1.2
1.0
0.8
0.6
0.4
-1.0
0
1.0
P = $P_e P_\gamma \cos\Psi$
2244A5

Figure 5

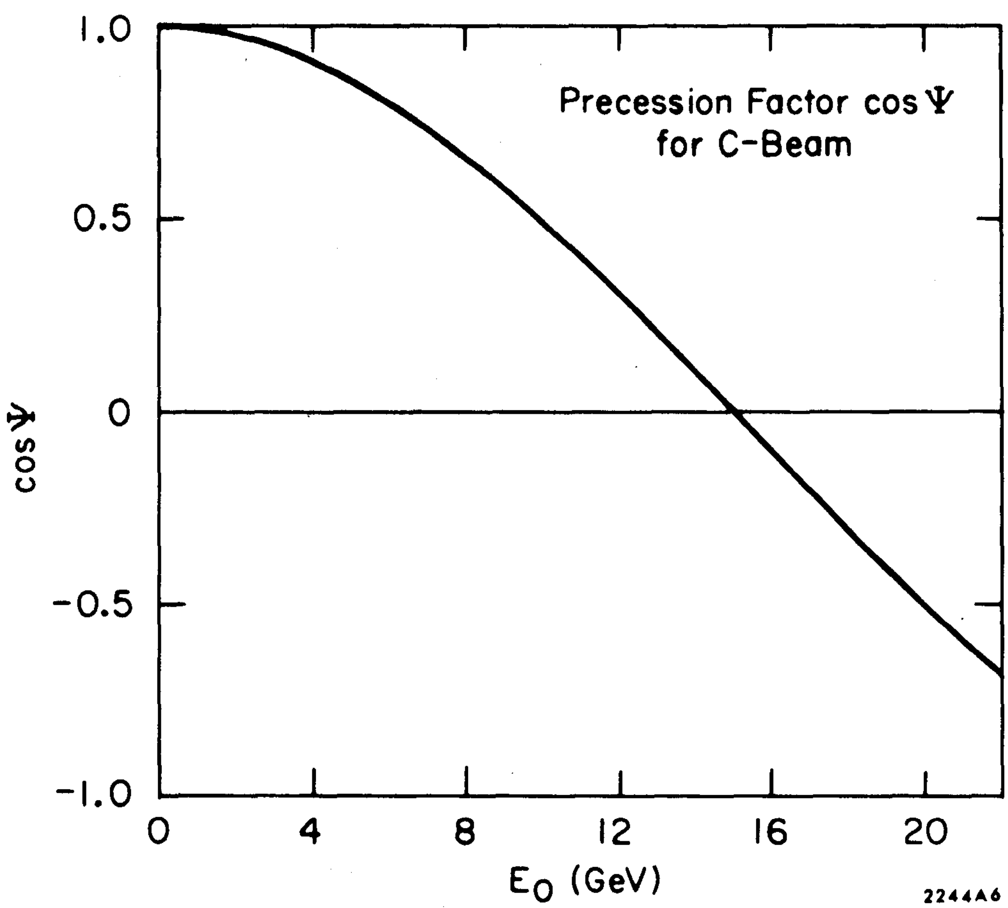
1.0
0.5
0
-0.5
-1.0
cos Ψ
0
4
8
12
16
20
E0 (GeV)
Precession Factor cos Ψ
for C-Beam
2244A6

Figure 6